Surfaces of percolation clusters in three dimensions

R. Mark Bradley
Department of Physics, Colorado State University, Fort Collins, Colorado 80523

P. N. Strenski
IBM Thomas J. Watson Research Center, Yorktown Heights, New York 10598

Jean-Marc Debierre
Laboratoire de Physique du Solide, Université de Nancy I, Boîte Postale 239, F-54506 Vandoeuvre-lès-Nancy, France

(Received 30 January 1991)

We present the results of a Monte Carlo study of the surfaces (or "hulls") of percolation clusters in three dimensions. The hulls were generated directly by a growing self-avoiding surface, called the smart kinetic surface, which is a generalization of the smart kinetic walk from two dimensions to three. We find that the fractal dimension of the hull at the percolation threshold is $D'=2.548\pm0.014$. Two other hull critical exponents were measured directly; we obtained $\tau'=2.19\pm0.01$ and $\gamma'=1.77\pm0.02$. These results are in accord with scaling laws which relate the hull exponents, and with a heuristic argument which suggests that the bulk and hull critical exponents are equal. The properties of percolation hulls determine the scaling behavior of transport, adsorption, and catalytic processes taking place at the surface of sintered metal powders.

I. INTRODUCTION

Percolation theory has applications in such diverse areas as electrical conduction in metal-insulator composites, fluid flow through porous media, gelation, and the spread of epidemics.[1] Much interest has centered on the structure of percolation clusters close to threshold, since this is where universal behavior emerges. Over the last decade, considerable progress has been made in determining the geometrical properties of percolation clusters in two dimensions (2D). In particular, the bulk[2] and surface[3] fractal dimensions have been determined exactly for the infinite cluster at threshold and are distinct. The exponents characterizing the divergence of the mean cluster size and the mean perimeter size are also known exactly.[2,3] The remaining geometrical exponents can be obtained via scaling relations.[1,4]

This analytical work has in large measure been stimulated by Monte Carlo results. In two dimensions, Monte Carlo studies of the cluster perimeters (or "hulls") have been greatly facilitated by the discovery of algorithms which allow the direct construction of cluster perimeters.[4–8] These algorithms use random walks to trace out the hulls and are vastly more efficient than the more obvious approach in which the lattice sites are randomly occupied with probability p, the clusters are identified, and finally the hulls are obtained.

Considerably less is known about percolation in three dimensions (3D). The bulk fractal dimension at threshold has been computed by Monte Carlo simulations and series expansions; the recent Monte Carlo results of Ziff and Stell[9] yield the value $D=2.529\pm0.016$, for instance. A rough estimate of the hull fractal dimension at the percolation threshold, D', has been made in the course of a study of "gradient percolation."[10] The result $D'\cong2.5$ does not rule out the possibility that the bulk and hull fractal dimensions differ in 3D as well as 2D.

The fractal dimension of the hull of the infinite cluster at threshold determines the scaling behavior of several directly measurable properties of disordered materials. For example, consider the problem of heat flow between liquid helium and a refrigerated metal. At low temperatures, there is a large acoustic mismatch between liquid helium and the metal, resulting in a substantial resistance to heat flow through the interface between these two materials.[11] This surface resistance is known as the Kapitza resistance and is the limiting factor in cooling ^{3}He and ^{4}He below 100 mK using a solid refrigerant. The usual method used to overcome this problem is to increase the interface area by employing a sintered metal powder. Measurements of the electrical conductivity and Young's modulus of sintered silver powders have been made over a range of metal fractions p by Deptuck, Harrison, and Zawadzki[12] and clearly indicate the presence of a percolation threshold at a critical value of p. These experiments also gave critical exponents for the behavior of the electrical conductivity and Young's modulus in the vicinity of the threshold, and these are in reasonable accord with the predictions of percolation theory. Thus, a sintered metal can be modeled as a percolation cluster. The interface area between a cubical sintered metal sample of side L and a bath of liquid helium will therefore scale as $(L/\xi)^2\xi^{D'}$, where the correlation length ξ diverges as $(p-p_c)^{-\nu}$ as p approaches the threshold metal fraction p_c. At ultralow temperatures, the bulk thermal resistances of the helium and metal can be neglected. Therefore, the resistance to heat flow goes to zero as $(p-p_c)^{(D'-2)\nu}$ as the metal fraction is reduced toward the

threshold value. We conclude that the value D' determines the scaling behavior of the resistance to heat flow at very low temperatures. The fractal dimension of the hull is also needed if we are to understand the scaling behavior of adsorption and surface-catalyzed reactions occurring at the surface of sintered metal powders.

In this paper we perform a Monte Carlo study of the surface geometry of percolation clusters in 3D. We introduce a technique in which the hulls are constructed directly by growing a random surface. The gain in computational efficiency obtained by direct construction of the hulls is even greater than in 2D and allows us to determine D' with considerably greater accuracy than in previous studies. We find that $D'=2.548\pm0.014$. The first estimates of two other hull critical exponents ($\tau'=2.19\pm0.01$ and $\gamma'=1.77\pm0.02$) are also obtained. Our values of the hull critical exponents are compared with recent estimates of the bulk critical exponents[8,13] and are consistent with the equality of the hull and bulk exponents. We also present a heuristic scaling argument which suggests that the hull and bulk exponents are identical. Finally, scaling relations among the various hull exponents are developed and tested.

The paper is organized as follows: In Sec. II we introduce our algorithm for the direct construction of percolation hulls in 3D. Our Monte Carlo results are presented in Sec. III. These results are discussed in Sec. IV, as are the scaling laws relating the hull exponents. We also give our heuristic argument for the equality of the bulk and hull critical exponents in Sec. IV. Our conclusions appear in Sec. V.

II. SMART KINETIC SURFACE

Our algorithm for generating percolation hulls in 3D is modeled on a procedure for directly constructing hulls in 2D. We will therefore briefly recall how 2D hulls can be produced by a self-avoiding random walk. For further details, we refer the reader to Refs. 4–8.

Procedures for the direct construction of percolation hulls have been established for both site and bond percolation on a variety of 2D lattices.[4–8] Here we will only consider site percolation on the triangular lattice,[6] since this is the closest analog to the problem we study in 3D. A hull of a percolation cluster is made up of bonds on the dual lattice that cut bonds joining unoccupied and occupied sites. A hull is a connected set of these bonds on the dual lattice. A given cluster has one external hull and may have one or more internal hulls.

The smart kinetic walk (SKW) traces out the hull of a site percolation cluster on the triangular lattice.[6] It is a kinetic self-avoiding walk on the dual lattice, which is hexagonal (Fig. 1). At the outset, the occupancy of sites on the original lattice is unspecified. The SKW begins by traversing a given bond on the dual lattice. The site on the original lattice to the right of the step is occupied, while the site to the left is unoccupied. The first step in the walk points toward a site on the original lattice. This site is now specified to be occupied with probability p or unoccupied with probability $1-p$. If the site is occupied, the walk turns left; otherwise, it turns right. The walk

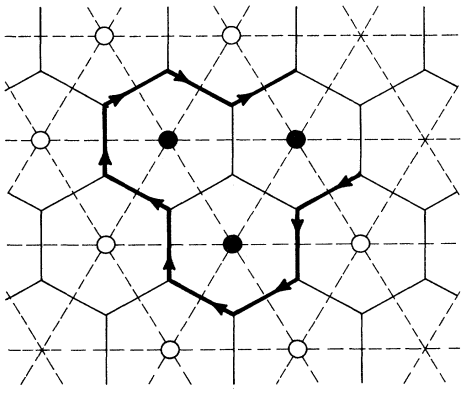

FIG. 1. SKW on the hexagonal lattice. The original triangular lattice is shown with dashed lines, while the dual hexagonal lattice is shown with solid lines. Solid and open circles at the vertices of the original lattice indicate sites which have been specified to be occupied or unoccupied, respectively. The SKW itself is shown with directed bold lines. This SKW occurs with probability $p^2(1-p)^6$.

now continues in this way. If at any time the last step of the walk points toward a site whose occupancy has already been specified, it turns left if the site is occupied and right if it is unoccupied. The walk ends when it returns to its point of origin.

This algorithm is particularly simple because the dual lattice is threefold coordinated, and this is the lowest coordination number a regular 2D lattice can have. In addition, each site on the dual lattice can only be visited once by the SKW. This is in contrast to the situation for site percolation on the square lattice. In that case, a site on the dual lattice can be shared by zero, two, or four bonds in the hull. As a result, it is possible to define two different hulls for site percolation on the square lattice.[14] One of these hulls has sites in the dual lattice that are shared by four hull bonds, while the other does not. This difference is significant, because these two hulls have different fractal dimensions. Site percolation on the triangular lattice is appealingly simple because there is only one possible definition of the hull.

The SKW is "smart" because it can only terminate by returning to its point of origin—it cannot enter a cul-de-sac from which there is no escape. The SKW is also strictly self-avoiding. Finally, note that these two observations can be combined into the single assertion that each site in the completed walk belongs to precisely two occupied bonds.

We now use these ideas as a basis for obtaining an algorithm for the direct construction of site percolation hulls in 3D. We consider two sites S and S' to be members of the same cluster only if there is a sequence of occupied sites $S,S_1,S_2,\ldots,S_n,S'$ in which each consecutive pair of sites are nearest neighbors. Since a percolation hull in 3D is a surface, we must seek a randomly growing surface, rather than a growing walk. Following the terminology used in 2D, we will call this randomly growing surface the smart kinetic surface (SKS). In 2D a percola-

tion hull is a set of bonds on the dual lattice. Equivalently, it is a set of edges of Wigner-Seitz (WS) cells. These edges form a closed loop in which each site belongs to an even number of occupied bonds. In three dimensions, the hull of a cluster will be a set of faces of WS cells. Each face in the hull belongs to two WS cells, one of which is centered on a site in the cluster. The site at the center of the other WS cell does not belong to the cluster. For brevity, we will refer to a face of a WS cell as a "plaquette" and to a plaquette in the hull as an "occupied plaquette." We will require the hull to be a closed surface in which each bond belongs to an even number of occupied plaquettes.

We elected to study site percolation on the body-centered-cubic (bcc) lattice. The WS cell of the bcc lattice is a truncated octahedron, which is a regular polyhedron with eight hexagonal faces and six square faces. The WS lattice is a space-filling packing of truncated octahedra, and a site of the original lattice resides at the center of each WS cell in the packing (Fig. 2). Note that each bond in the WS lattice is shared by two hexagonal faces and one square face. Hexagonal faces of the WS lattice bisect bonds between nearest-neighbor (NN) pairs of sites in the original lattice, while square faces lie between next-nearest-neighbor (NNN) sites.

The bcc lattice was chosen because its WS lattice is fourfold coordinated, and this is the lowest coordination number a 3D lattice can have. Moreover, each bond in the WS lattice either does not belong to a hull or is shared by two plaquettes in a hull. This is simpler than the situation for the simple cubic lattice. Bonds in the WS lattice of the simple cubic lattice can be shared by zero, two, or four plaquettes in hulls, and thus there is more than one possible definition of the hull, just as in the case of the 2D square lattice.[14]

Before describing our algorithm, we introduce a convenient labeling scheme. As noted above, a plaquette belongs to two WS cells. Let the sites at the center of these cells be sites S_1 and S_2, respectively. Clearly, the pair (S_1,S_2) uniquely labels the plaquette. (Sites S_1 and S_2 are NN's for hexagonal plaquettes and are NNN's for square plaquettes.) Now consider one of the bonds on the perimeter of the plaquette (S_1,S_2). This bond is shared by three plaquettes, labeled (S_1,S_2),(S_1,S_3), and (S_2,S_3). Accordingly, we label the bond by the *unordered* triplet (S_1,S_2,S_3).

It will also be helpful to make some definitions before stating the growth rules for the SKS. A site on the original lattice will be said to be "black" if it is occupied and "white" if it is unoccupied. Accordingly, we say that a site is colored if its occupancy has been specified; otherwise, it is uncolored. An "edge" of the SKS is defined to be a bond in the WS lattice that belongs to one occupied plaquette. Less formally, an edge is a bond on the perimeter of the SKS. Consider an edge of the growing SKS that belongs to the occupied plaquette (S_1,S_2) and which is shared by the unoccupied plaquettes (S_2,S_3) and (S_1,S_3). As will be seen when we define the SKS, one of the sites S_1 and S_2 must be black and the other white. We will take S_1 to be occupied and S_2 to be unoccupied, and label the edge by the *ordered* triplet $[S_1,S_2,S_3]$. (We will enclose ordered triplets with square brackets to distinguish them from unordered triplets.) We now classify this edge as being "active" or "inactive". The edge is active if sites S_1 and S_3 are NN's and is inactive if they are NNN's. Hexagonal plaquettes may have both active and inactive edges (Fig. 3), whereas square plaquettes cannot have inactive edges.

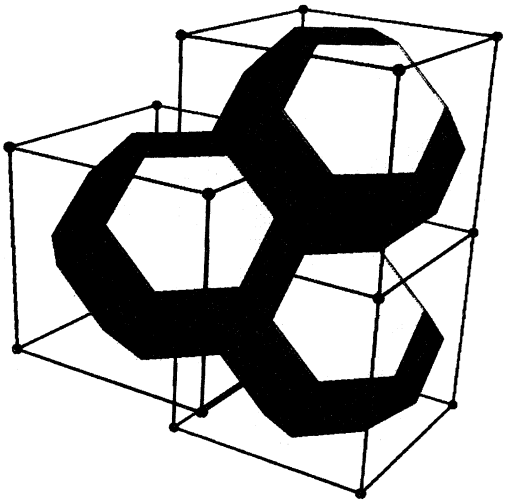

FIG. 2. Wigner-Seitz lattice for the bcc lattice. The sites of the bcc lattice (solid circles) form two interpenetrating simple cubic lattices. The Wigner-Seitz lattice is a space-filling package of truncated octahedra (shaded solids). A site of the bcc lattice resides at the center of each truncated octahedron.

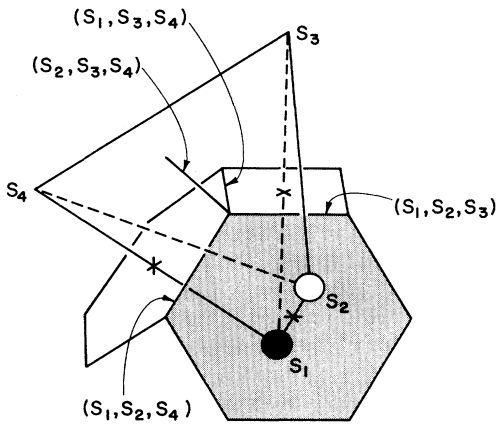

FIG. 3. Active and inactive edges of an occupied hexagonal plaquette. Sites S_1, S_2, S_3, and S_4 are sites belonging to the original bcc lattice. S_1 is black and S_2 is white. A solid (dashed) line between two sites of the bcc lattice represents a NN (NNN) bond in the original lattice. The plaquettes (S_1,S_2), (S_1,S_3), and (S_1,S_4) are shown. The shaded plaquette (S_1,S_2) is occupied. The points where bonds of the bcc lattice intersect plaquettes are shown with crosses. The bond (S_2,S_3,S_4) is also shown. If sites S_3 and S_4 are uncolored, the edge $[S_1,S_2,S_3]$ is inactive and the edge $[S_1,S_2,S_4]$ is active.

The growth of the SKS proceeds as follows: We begin with a NN pair of sites, one colored black and the other white. The hexagonal plaquette between these two sites is occupied. All other sites in the original lattice are initially uncolored, and the remaining plaquettes are unoccupied. Now consider the growth of the SKS after an arbitrary number of plaquettes have been added sequentially to its perimeter. We choose one of the active edges at random. Following the notation introduced in the previous paragraph, we label this edge using the ordered triplet $[S_1,S_2,S_3]$. If site S_3 is uncolored, it is colored black with probability p and white with probability $1-p$. If S_3 is already colored, its coloring is left unchanged. The plaquette (S_2,S_3) is now occupied if site S_3 is black. If S_3 is white, the plaquette (S_1,S_3) is occupied. In either case, the edges of the newly occupied plaquette must be added to or removed from the lists of active and inactive edges. Another active edge is now chosen at random, and another plaquette is occupied using the rules just stated. The growth process continues until there are no more active edges remaining.

When all the active edges have been exhausted, inactive edges may remain. If there are any such inactive edges, they must occur in sets of four that surround square plaquettes, as will be shown in the next paragraph. These plaquettes are now occupied. This final "patch-up" phase of the SKS algorithm yields a closed surface of occupied plaquettes in which each bond is shared by precisely two occupied plaquettes. The SKS is therefore both "smart" and self-avoiding.

To see that the remaining inactive edges must occur in square loops of four, consider a particular inactive edge, labeled $[S_1,S_2,S_3]$ (Fig. 3). This is an edge of the square plaquette (S_1,S_3). Let site S_4 be one of the two sites which is a NN of sites S_1 and S_3 and a NNN of site S_2. The edge in question must belong to a closed loop of inactive edges because no active edges remain. Thus one of the bonds (S_1,S_3,S_4), (S_2,S_3,S_4), or (S_1,S_2,S_4) must belong to the loop. We claim that it is in fact the first of these bonds that is in the loop. Since sites S_1 and S_4 are NN's, the edge $[S_1,S_2,S_4]$ cannot be an inactive edge and does not belong to the loop. Since this edge cannot be active either, the bond (S_1,S_2,S_4) must be shared by two occupied plaquettes and site S_4 must have been colored during the growth of the SKS. If S_4 is white, the edge $[S_1,S_4,S_3]$ is inactive, as claimed. If S_4 is black, the edge $[S_4,S_2,S_3]$ cannot be inactive since sites S_4 and S_3 are NN's. The bond (S_1,S_3,S_4) must therefore be an inactive edge, and the claim is established. Applying this argument twice more, we see that all four bonds on the perimeter of the square (S_1,S_3) must be inactive edges, as required.

We now show that the SKS generates the hull of a site percolation cluster on the bcc lattice. More precisely, we will demonstrate that the probability that the SKS generates a particular closed surface configuration C is equal to $p^{-1}(1-p)^{-1}\pi(C)$ where $\pi(C)$ is the probability that a given hexagonal plaquette is contained in the hull configuration C in site percolation on the bcc lattice. Consider the active edge $[S_1,S_2,S_3]$. If site S_3 is uncolored, it is colored black or white with the appropriate probabilities. If S_3 has already been colored, its color is left unchanged. If S_3 is white, the hull must cut the NN bond between sites S_1 and S_3. Accordingly, the plaquette (S_1,S_3) is occupied. If S_3 is black, the occupied NN sites S_1 and S_3 are members of the same cluster. The hull therefore cannot cut the bond between S_1 and S_3. By definition, the completed hull can have no edges, and so the plaquette (S_2,S_3) is now occupied.

Growth cannot occur at inactive edges in our definition of the SKS. The reason we adopt this rule is that sites 1 and 3 are NNN's in this case, and occupied NNN sites may or may not be in the same cluster. Any inactive edges remaining at the end of the growth process are instead dealt with in the patch-up phase.

Now consider the effect of the patch-up phase. Once the active edges have been exhausted and growth has ceased, we are left with a connected sheet composed of hexagonal and square faces. Consider an arbitrary plaquette (S_1,S_2) in the sheet, and take S_1 to be inside the hull. Site S_1 is black and site S_2 is white if the sheet is an external hull. If the sheet is an internal hull, on the other hand, S_1 is white and S_2 is black. As shown above, the sheet can have holes in it, but these must be square plaquettes with four inactive edges. Consider one such plaquette, labeled (S_3,S_4). Sites S_3 and S_4 cannot both be white—at least one of these sites must be black. Suppose S_3 is black. S_4 cannot be a member of the cluster, since there is no path of occupied NN sites joining it to S_3. (Note, in particular, that S_3 and S_4 are NNN's.) Therefore, the plaquette (S_3,S_4) belongs to the hull and must be occupied. This is just what is done in our patch-up phase. We conclude that the SKS does indeed produce the hull of a site percolation cluster on the bcc lattice.

III. RESULTS

We constructed 30 000 SKS's at each of the following p values: $p=0.115$, 0.165, 0.195, 0.215, 0.22, 0.23, 0.235, 0.24, 0.245, 0.2455, 0.246, 0.2465, and 0.247. If a SKS still had active edges remaining when 5000 sites had been colored black, the growth process was terminated and the sheet was left open. On the other hand, if all active edges were exhausted when fewer than 5000 sites had been colored black, the sheet was closed in the "patch-up" phase.

At the percolation threshold $p=p_c$, the fraction of hulls that have N neighboring occupied sites scales as $N^{-\tau'}$. Thus the fraction $F(N)$ of SKS's which have N or more black sites must scale as $N^{2-\tau'}$. Close to the percolation threshold, $F(N)$ has the scaling form[1,4]

$$F(N)=F_\infty(p)+N^{2-\tau'}f(|p-p_c|N^{\sigma'}) . \tag{3.1}$$

The scaling function $f(x)$ approaches a finite, nonzero constant as $x\to 0$ and decays exponentially to zero as $x\to\infty$. $F_\infty(p)$ is the fraction of SKS's that grow to infinite size and is nonzero for $p_c<p<1-p_c$ because the hull of the infinite cluster has fractal dimension 3 in this regime.[10,15] $F_\infty(p)$ is zero for $p\le p_c$ and $p\ge 1-p_c$.

Figure 4 is a log-log plot of $F(N)$ for several values of

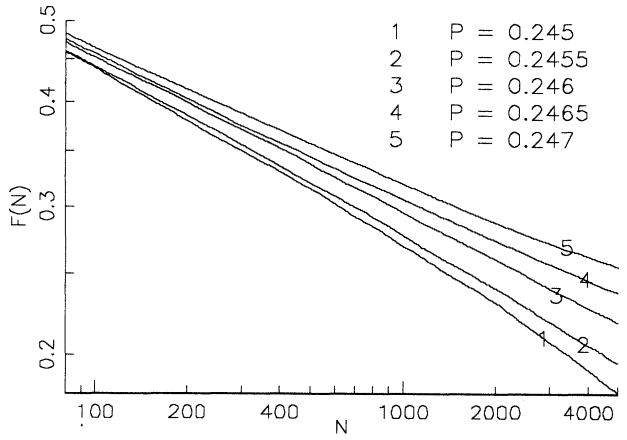

FIG. 4. Log-log plot of the fraction $F(N)$ of SKS's which have N or more black sites vs N. Results are shown for $p=0.245$, 0.2455, 0.246, 0.2465, and 0.247.

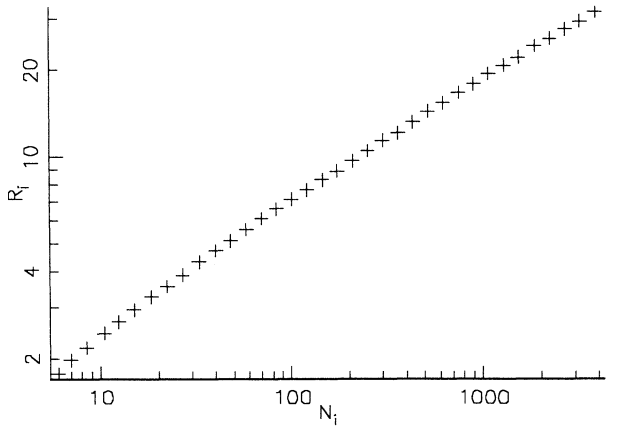

FIG. 5. Log-log plot of the mean radius of gyration of a closed SKS in the ith bin (R_i) vs the mean number of black sites in a sheet in the bin (N_i).

p. The plot for $p=0.246$ is very close to being straight, and the deviations from linearity are comparable in size to the statistical errors. On the other hand, the plots for $p \leq 0.2455$ and $p \geq 0.2465$ have small but discernible curvatures. We therefore adopt $p_c=0.2460\pm0.0003$ as our best estimate of the percolation threshold for site percolation on the bcc lattice.[16] Our result is in good agreement with the result obtained by Gaunt and Sykes[17] using a low-density series expansion $p_c=0.2464\pm0.0007$. Both our result and that of Gaunt and Sykes are consistent with the estimate of Sykes, Gaunt, and Glen,[18] $p_c=0.245\pm0.004$.

A straight-line fit to the log-log plot of $F(N)$ versus N was performed at $p=0.246$. The first 200 values of N were omitted in producing this fit, since the log-log plot deviates significantly from linearity in this regime. This yielded the estimate $\tau'=2.1884\pm0.0005$ for the exponent τ'. The uncertainty in this estimate is the error in the least-squares fit and does not take into account the uncertainty in the value of p_c. To gauge the size of the error in τ' coming from the latter source, we carried out least-squares fits to the linear portions of the log-log plots of $F(N)$ at $p=0.2455$ and 0.2465. We found that the uncertainty in p_c is the dominant source of error in our estimate of τ'. Our final estimate of the exponent τ' is $\tau'=2.19\pm0.01$.

We next computed the fractal dimension of the closed and open SKS's at the threshold. Let us first consider the results for the closed sheets. Because there was a comparatively small number of large sheets, the data were binned as follows. A closed SKS with N black sites belongs to the ith bin if

$$n_i \leq N < n_{i+1} , \tag{3.2}$$

where $n_i \equiv [5(1.2)^i]$ and $[x]$ is the least integer greater than or equal to x. The mean number of black sites in a sheet lying in the ith bin will be denoted by N_i, while the mean radius of gyration of a SKS in this bin will be denoted by R_i. A log-log plot of N_i versus R_i is shown in Fig. 5. The small but appreciable curvature present in this plot indicates that a finite-size analysis is needed to obtain an accurate estimate of the fractal dimension. We assume that the corrections to scaling have the form

$$N = AR^{D'}(1+BR^{-1}+CR^{-\Delta}+\cdots) , \tag{3.3}$$

where A, B, C, and Δ are constants. We next define the finite-size estimator

$$D_i' = \frac{\ln N_{i+4} - \ln N_{i-4}}{\ln R_{i+4} - \ln R_{i-4}} . \tag{3.4}$$

Employing the finite-size ansatz (3.3), we see that for large i the estimator D_i' scales as

$$D_i' \cong D' - BR_i^{-1} - \Delta CR_i^{-\Delta} + \cdots , \tag{3.5}$$

provided that $0<\Delta\leq 2$. Our data for D_i' are plotted versus R_i^{-1} in Fig. 6. Extrapolation to the limit $R^{-1}=0$

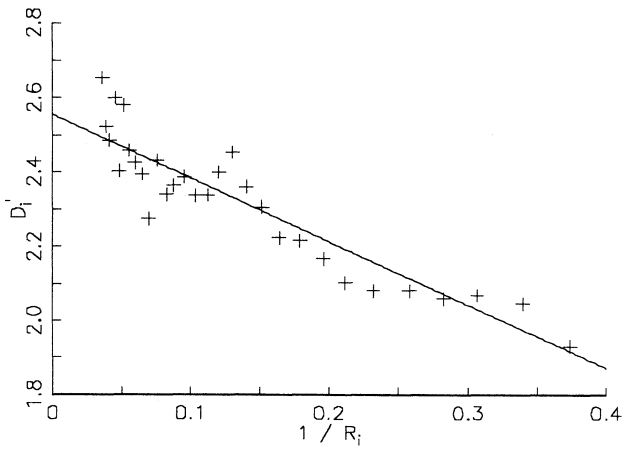

FIG. 6. Finite-size estimator D_i' for the fractal dimension of closed SKS's plotted vs $1/R_i$ (crosses). R_i is the mean radius of gyration of a closed SKS in the ith bin. The linear least-squares fit to the data is also shown (solid line). This fit yields the estimate $D'=2.548\pm0.014$ for the fractal dimension of the closed SKS's.

is problematic in models with $\Delta < 1$, but a simple linear fit works well here, indicating that Δ is probably greater than 1. Accordingly, we performed a least-squares fit to the form (3.5) with $C=0$ and so obtained the estimate $D'=2.548\pm0.014$ for the fractal dimension of percolation hulls in 3D. Our result is comparable to the rough estimate $D'\simeq 2.5$ obtained by Gouyet and co-workers in their study of gradient percolation in 3D.[10,15]

We next turn to the open sheets. Consider the growth of a particular sheet. At each time step, we computed the number of sites colored black (N) and the radius of gyration of those sites. If N satisfied the inequality (3.2), the SKS was classified as a member of the ith bin at this time step, and N was added to a running total of the number of black sites in this bin, T_i. The radius of gyration of the sheet was also added to a running total of radii for this bin, Σ_i. Once all 30 000 sheets had been grown, we computed the number of entries E_i in each bin. The mean number of black sites in a SKS in the ith bin was defined to be $N_i^{\text{open}} \equiv T_i/E_i$, and the mean radius of gyration of a sheet in this bin is $R_i^{\text{open}} \equiv \Sigma_i/E_i$. The finite-size estimator (3.4) was then computed with N_i and R_i replaced by N_i^{open} and R_i^{open}, respectively. Our data for D_i' are plotted versus $1/R_i^{\text{open}}$ in Fig. 7. A linear least-squares fit to the data (omitting the points with $1 \le i \le 10$) yields the estimate $D'_{\text{open}}=2.544\pm0.002$ for the fractal dimension of the open sheets. The uncertainty quoted here is simply the error in the least-squares fit and does not take into account the uncertainty in the value of p_c or possible difficulties with the finite-size extrapolation.

This result warrants some discussion. We showed in Sec. II that the SKS constructs the hull of a percolation cluster. Thus a closed sheet has the same fractal dimension as the hull. An open sheet need not have the same fractal dimension as the hull because it could spread out rapidly over the cluster's surface, leaving large regions uncovered. Since a particular open sheet is a subset of a hull, however, we must have $D'_{\text{open}} \le D'$, and so our computation of D'_{open} gives us a lower bound on D'. This lower bound is consistent with our result $D'=2.548\pm0.014$.

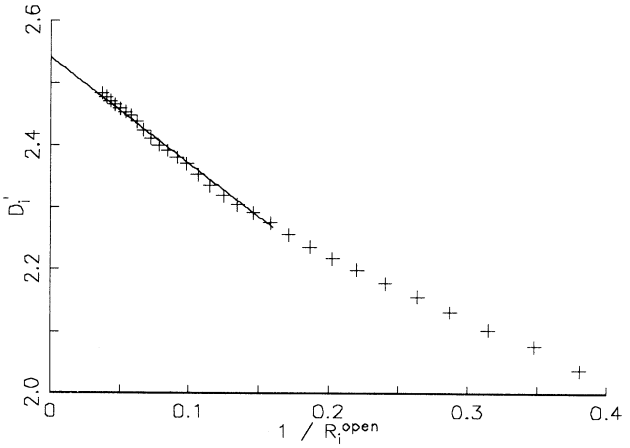

FIG. 7. Finite-size estimator D_i' for the fractal dimension of open SKS's plotted vs $1/R_i^{\text{open}}$. R_i^{open} is the mean radius of gyration of an open SKS in the ith bin. Also shown is a linear least-squares fit to the data with $i > 10$ (solid line). This fit gives the estimate $D'_{\text{open}}=2.544\pm0.002$ for the fractal dimension of the open SKS's.

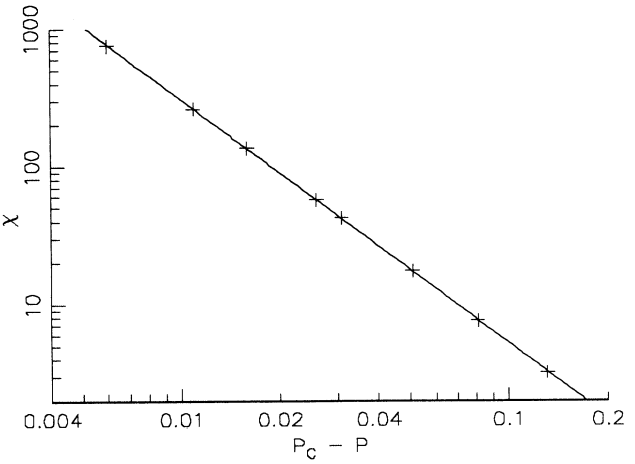

FIG. 8. Log-log plot of the mean number of occupied sites in a hull (χ) vs $p_c - p$. The data points are indicated with crosses. The linear least-squares fit to the data is shown using a solid line. This fit yields the estimate $\gamma'=1.77\pm0.02$ for the exponent γ'.

Next, consider the behavior of the hulls for $p < p_c$. The mean number of occupied sites in a hull, χ, diverges as p approaches p_c. For p close to the threshold, $\chi \sim (p_c - p)^{-\gamma'}$. The critical exponents τ', γ', and σ' are related through the scaling relation

$$\gamma' = (3-\tau')/\sigma' \ . \tag{3.6}$$

This relationship is readily derived using the scaling form for $F(N)$ [Eq. (3.1)].

The mean number of black sites in the SKS's, $\langle N \rangle$, was computed for each value of $p < p_c$ we studied. For the p values 0.115, 0.165, 0.195, 0.215, 0.22, and 0.23, no open sheets remained when the cutoff size of 5000 black sites was reached. Thus $\langle N \rangle$ should provide a good estimate for χ for these values of p. At the points $p=0.235$ and 0.24, on the other hand, an appreciable proportion of SKS's still had active edges when the cutoff was reached. For these values of p, we performed an exponential fit to the tail of $F(N)$ and used this to extrapolate $F(N)$ to values of N greater than 5000. Our data for $F(N)$ were then used for the first 5000 terms in the sum $\chi = \sum_{N=1}^{\infty} F(N)$, and the extrapolated values were employed for the remainder. Although the exponential fit to the tail of $F(N)$ worked well at $p=0.235$ and 0.24, it was not sufficiently accurate to be used at $p=0.245$ and 0.2455. Figure 8 is a log-log plot of our data for χ as a function of $p_c - p$. A linear least-squares fit to the data yields the estimate $\gamma'=1.77\pm0.02$. The error quoted in this estimate is due almost entirely to the uncertainty in the value of p_c.

Let $P_i \equiv [F(n_i) - F(n_{i+1})]/(n_i - n_{i+1})$ be the probability that a closed SKS lies in the ith bin, divided by the length of the bin. From Eq. (3.1) we have the following

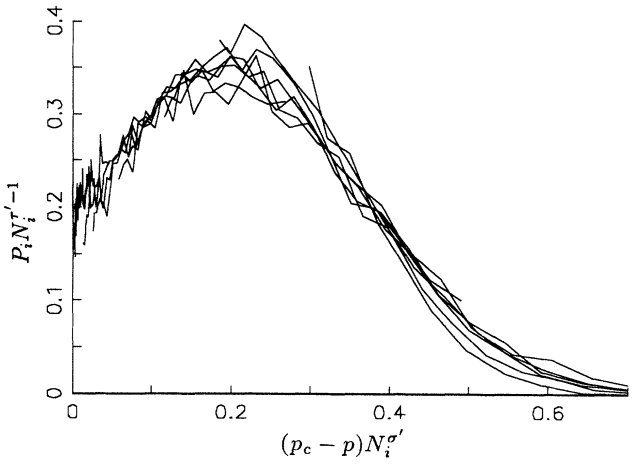

FIG. 9. Scaling plot of P_i. The quantity $P_i N_i^{\tau'-1}$ is plotted vs $(p_c-p)N_i^{\sigma'}$ for $p=0.115$, 0.165, 0.195, 0.215, 0.22, 0.23, 0.235, 0.24, 0.245, and 0.2455.

scaling form for P_i:

$$P_i \sim N_i^{1-\tau'} g(|p-p_c|N_i^{\sigma'}) . \tag{3.7}$$

Here $g(x)$ is a scaling function which decays exponentially for large x and tends to a nonzero constant as $x \to 0$. To test this scaling form, the estimate $\sigma' \cong 0.46$ was obtained from Eq. (3.6) and our computed values of τ' and γ'. We then plotted $P_i N_i^{\tau'-1}$ versus $|p-p_c|N_i^{\sigma'}$ for several values of p (Fig. 9). These plots fall on a common curve to a good approximation, and thus our estimates of the value of p_c and the hull critical exponents seem to be consistent.

IV. DISCUSSION

Just as in the case of 2D percolation hulls,[4] several scaling laws can be derived which relate the exponents characterizing 3D hull percolation hulls. We have already given one such scaling relation [Eq. (3.6)]. We now construct two more.

Consider site percolation in d dimensions at the percolation threshold $p=p_c$. The average number of hulls with N black sites lying within a hypercubical volume of side L will be denoted by $\Omega(N)$. If L and N are large, but $N \ll L^d$, then $\Omega(N) \sim L^d N^{-\tau'}$. Conversely, the number of sites in a hull that lies entirely within the volume cannot exceed L^d, and so $\Omega(N)=0$ for $N > L^d$. We now combine these two observations to give the scaling form $\Omega(N)=N^{-\tau'+1}h(N/L^d)$ which holds for arbitrary large N and L. The scaling function $h(x)$ diverges as x^{-1} for small x and is zero for $x>1$. At the percolation threshold, at least one cluster spans the system; thus, at least one hull must extend across the volume. More precisely, the number of clusters—and hence the number of hulls—that span the system must be of order 1. A typical hull which extends across the volume contains at least $L^{D'}$ black sites, since the hull fractal dimension is D'. Thus, employing our scaling form for $\Omega(N)$, we see that the number of hulls which span the volume scales as

$$\sum_{N=L^{D'}}^{\infty} \Omega(N) \sim L^{d+(1-\tau')D'} .$$

As already noted, this number must be of order 1; i.e., it scales as L^0. We therefore have the scaling law

$$\tau' = \frac{d}{D'} + 1 , \tag{4.1}$$

a relation first written down by Ziff for percolation hulls in 2D.[4] Employing our measured value of D' in dimension $d=3$, we have $d/D'+1=2.177\pm0.007$. This is in reasonable agreement with our estimate $\tau'=2.19\pm0.01$, and so our values for D' and τ' are consistent with this scaling relation.

The scaling form for $P(N)$ [Eq. (3.7)] shows that the number of black sites in the hull of a typical finite cluster scales as $|p-p_c|^{-1/\sigma'}$ for p close to p_c. This number also scales as $\xi^{D'} \sim |p-p_c|^{-D'\nu}$, since the correlation length ξ is the typical linear dimension of a finite cluster. We therefore have a third scaling relation,

$$\sigma' = \frac{1}{D'\nu} . \tag{4.2}$$

Combining this with Eq. (3.6) yields

$$\nu = \frac{\gamma'}{(3-\tau')D'} . \tag{4.3}$$

Inserting our measured values of D', τ', and γ' into this relation, we obtain the estimate $\nu=0.86\pm0.03$ for the exponent ν in dimension $d=3$. Our value for ν is in agreement with the most recent Monte Carlo estimate $\nu=0.875\pm0.008$,[9] and with the most recent series value $\nu=0.872\pm0.070$.[13,19]

The Monte Carlo results of Ziff and Stell[9] give the bulk exponent values $D=2.529\pm0.016$, $\tau=2.186\pm0.008$, and $\gamma=1.795\pm0.005$. Similarly, the recent series expansion study of Adler *et al.*[13] yielded $D=2.54\pm0.07$, $\tau=2.18\pm0.03$, and $\gamma=1.805\pm0.020$. In both cases, the results lie within the error bars of our values for D', τ', and γ'.[19] In the following, we will advance heuristic arguments which suggest that the bulk and hull critical exponents are in fact identical.

We begin by presenting an argument for the equality of the bulk and hull fractal dimensions that is valid for $p_c \le p < 1-p_c$.[20] We say that a site is in the "perimeter" of a black cluster if it is white and is a NN of a site in the cluster. Let t_s be the average number of sites in the perimeter of a cluster of s sites. For large s, the ratio t_s/s tends to $(1-p)/p$.[21] Since the lattice coordination number z is finite, this means that a nonzero fraction of sites in the infinite cluster of black sites are NN's of perimeter sites. Now $p < 1-p_c$, and so a white site has a nonzero probability of belonging to the infinite cluster of white sites. It is therefore plausible that a nonzero fraction of the perimeter sites belong to the infinite cluster of white sites. If this is so, a finite fraction of the sites in the infinite cluster of black sites belongs to its external surface, and the hull and bulk fractal dimensions must coincide for $p_c \le p < 1-p_c$. In particular, D and D' must be equal, and the fractal dimension of the hull is 3 for $p_c < p < 1-p_c$.

This argument is not rigorous because a perimeter site is less likely to belong to the infinite cluster of white sites than an arbitrarily chosen white site. In fact, the fraction of perimeter sites that belong to the infinite cluster of white sites could vanish in the thermodynamic limit. However, note that for $p \geq p_c$, the probability of growing even a small internal hull is minute. For example, the probability of growing an internal hull which is a truncated octahedron of 14 faces is p^{13}. At $p = p_c$, this probability is roughly 1.2×10^{-8}. The vast majority of the perimeter therefore belongs to the external hull, and we again arrive at the conclusion $D = D'$.

An ordinary critical point is characterized by two independent critical exponents. Thus, the exponents D' and γ' are sufficient to describe the critical properties of the hull. Let us suppose that D and D' are in fact equal. Since $\gamma = (2D - d)\nu$ and $\gamma' = (2D' - d)\nu$, the exponents γ and γ' would then be equal as well. All the exponents characterizing the hull would therefore be identical to their bulk counterparts. As noted above, this conclusion, although not based on rigorous arguments, is consistent with our Monte Carlo results.

We close by comparing the properties of hulls at the percolation threshold to those of other random self-avoiding surfaces. Random self-avoiding surfaces composed of plaquettes embedded in a regular 3D lattice arise naturally in the high-temperature expansion of lattice gauge theories[22] and have been studied using the exact enumeration method.[23] These surfaces are believed to belong to the same universality class as lattice animals,[24] which have fractal dimension 2 in three dimensions.[25] Kantor, Kardar, and Nelson introduced a model for the equilibrium behavior of a polymerized membrane, the "tethered surface."[26] In contrast to the plaquette model, the internal connectivity is fixed in a tethered surface. Flory theory arguments and initial Monte Carlo results both suggested a fractal dimension of 2.5 for tethered surfaces.[26] However, more extensive Monte Carlo work[27–29] and molecular-dynamics simulations[30] indicate that these membranes are probably rough but flat and so have an asymptotic fractal dimension of 2. Both of these models of the equilibrium properties of self-avoiding membranes appear to have scaling properties which differ from those of percolation hulls at threshold. Fluid vesicles have been predicted to have a high-temperature crumpled phase,[31,32] and recent Monte Carlo simulations[29] give a nontrivial fractal dimension of 2.5 in this regime, in agreement with these predictions. The intriguing possibility that athermal fluid vesicles have a fractal dimension equal to D' cannot be ruled out at this time. Finally, note that we constructed our percolation hulls using the SKS, which is a growing self-avoiding surface. Only two other models of growing self-avoiding surfaces have previously been studied,[33] and these models both appear to have fractal dimensions which differ from that of the SKS.

V. CONCLUSIONS

In this paper we reported the results of a Monte Carlo study of percolation hulls in 3D. Hulls of site percolation clusters on the bcc lattice were generated directly using a growing self-avoiding surface, the smart kinetic surface. The SKS is a considerably more efficient method of producing hulls than the most obvious approach in which all the lattice sites are randomly occupied, the clusters are identified, and finally the hulls are obtained. We find that the fractal dimension of the hull at the percolation threshold is $D' = 2.548 \pm 0.014$. We also obtained the hull exponent estimates $\tau' = 2.19 \pm 0.01$ and $\gamma' = 1.77 \pm 0.02$, and the value $p_c = 0.2460 \pm 0.0003$ for the site percolation threshold on the bcc lattice. Three scaling laws which relate the hull exponents were proposed and found to be consistent with our estimates of the exponents. Our values of the hull critical exponents were compared with bulk critical exponents obtained in the most recent Monte Carlo and series-expansion studies and are consistent with the equality of the hull and bulk exponents. Finally, heuristic, nonrigorous arguments were advanced which suggest that the hull and bulk exponents are indeed identical.

As discussed in the Introduction, the critical properties of percolation hulls determine the scaling behavior of heat transport between sintered metal powders and liquid helium at temperatures below 100 mK. The behavior of percolation hulls near threshold is also relevant to adsorption and catalytic processes taking place at the surface of sintered metal powders. In the broadest context, our work should apply to processes occurring at the surface of a porous random medium when the medium is close to its percolation threshold. We hope that this work will stimulate experimental work on this fascinating class of problems.

ACKNOWLEDGMENTS

We would like to thank Cliff Pickover for assistance with the graphics. One of us (R.M.B.) wishes to express his gratitude to the IBM Corporation and to the Polymeric Materials Center of the Colorado Advanced Materials Institute for partial support of this work.

[1] D. Stauffer, *Introduction to Percolation Theory* (Taylor and Francis, London, 1985).

[2] B. Neinhuis, J. Stat. Phys. **34**, 731 (1984); in *Phase Transitions and Critical Phenomena,* edited by C. Domb and J. L. Lebowitz (Academic, New York, 1987), Vol. 11.

[3] H. Saleur and B. Duplantier, Phys. Rev. Lett. **58**, 2325 (1987); B. Duplantier, Physica D **38**, 71 (1989); Phys. Rep. **184**, 229 (1989).

[4] R. M. Ziff, Phys. Rev. Lett. **56**, 545 (1986).

[5] R. M. Ziff, P. T. Cummings, and G. Stell, J. Phys. A **17**, 3009 (1984).

[6] A. Weinrib and S. A. Trugman, Phys. Rev. B **31**, 2993 (1985).

[7] J. M. F. Gunn and M. Ortuno, J. Phys. A **18**, L1095 (1985); P. Grassberger, *ibid.* **19**, 2675 (1986).

[8]R. M. Ziff, Physica D **38**, 377 (1989).
[9]R. M. Ziff and G. Stell (unpublished).
[10]J.-F. Gouyet, M. Rosso, and B. Sapoval, Phys. Rev. B **37**, 1832 (1988).
[11]E. T. Swartz and R. O. Pohl, Rev. Mod. Phys. **61**, 605 (1989).
[12]D. Deptuck, J. P. Harrison, and P. Zawadzki, Phys. Rev. Lett. **54**, 913 (1985).
[13]J. Adler, Y. Meir, A. Aharony, and A. B. Harris, Phys. Rev. B **41**, 9183 (1990).
[14]T. Grossman and A. Aharony, J. Phys. A **19**, L745 (1986); **20**, L1193 (1987); S. S. Manna, *ibid.* **22**, 433 (1988); M. Kolb, Phys. Rev. A **41**, 5725 (1990).
[15]M. Rosso, J.-F. Gouyet, and B. Sapoval, Phys. Rev. Lett. **57**, 3195 (1986).
[16]Throughout the paper the error bars will signify a 68% confidence interval.
[17]D. S. Gaunt and M. F. Sykes, J. Phys. A **16**, 783 (1983).
[18]M. F. Sykes, D. S. Gaunt, and M. Glen, J. Phys. A **9**, 1705 (1976).
[19]For a comprehensive review of numerical estimates of the bulk percolation exponents, see Ref. 13.
[20]An argument of this kind appears on p. 60 of Ref. 1, but its regime of validity is restricted to $p_c < p < 1-p_c$. The argument given here is a refinement and a generalization of that given in Ref. 1. Note that our argument does not imply that the bulk and hull fractal dimensions are the same in 2D, since $p_c \geq \frac{1}{2}$ for planar lattices [see, for example J. M. Ziman, *Models of Disorder* (Cambridge University Press, Cambridge, England, 1979), pp. 375–376].
[21]Reference 1, pp. 59–60.
[22]R. Balian, J. M. Drouffe, and C. Ityzkson, Phys. Rev. D **11**, 2104 (1975).
[23]S. Redner, J. Phys. A **18**, L723 (1985); **19**, 3199 (1986).
[24]B. Durhuus, J. Frolich, and T. Johnsson, Nucl. Phys. **B240**, 453 (1984); U. Glaus, Phys. Rev. Lett. **56**, 1996 (1986); J. Stat. Phys. **50**, 1141 (1988).
[25]G. Parisi and N. Sourlas, Phys. Rev. Lett. **46**, 871 (1981).
[26]Y. Kantor, M. Kardar, and D. R. Nelson, Phys. Rev. Lett. **57**, 791 (1986); Phys. Rev. A **35**, 3056 (1987).
[27]M. Plischke and D. Boal, Phys. Rev. A **38**, 4943 (1988); D. Boal, E. Levinson, D. Liu, and M. Plischke, *ibid.* **40**, 3292 (1989).
[28]J.-S. Ho and A. Baumgartner, Phys. Rev. Lett. **63**, 1324 (1989).
[29]A. Baumgartner and J.-S. Ho, Phys. Rev. A **41**, 5747 (1990).
[30]F. F. Abraham, W. E. Rudge, and M. Plischke, Phys. Rev. Lett. **62**, 1757 (1989).
[31]W. Helfrich, J. Phys. (Paris) **46**, 1263 (1985).
[32]L. Peliti and S. Leibler, Phys. Rev. Lett. **54**, 1690 (1985).
[33]J.-M. Debierre and R. M. Bradley, J. Phys. A **22**, L213 (1989).